

Upson SJ, OHaire T, Russell SJ, Dalgarno K, Ferreira AM. [Centrifugally Spun PHBV Micro and Nanofibres](#). *Materials Science & Engineering C* 2017, 76, 190-195.

**Copyright:**

© 2017 The Authors. Published by Elsevier B.V. Open Access funded by Engineering and Physical Sciences Research Council under a Creative Commons [license](#)

**DOI link to article:**

<http://dx.doi.org/10.1016/j.msec.2017.03.101>

**Date deposited:**

17/03/2017



This work is licensed under a [Creative Commons Attribution 4.0 International License](#)



# Centrifugally spun PHBV micro and nanofibres



Sarah J Upson<sup>a</sup>, Tom O'Haire<sup>b</sup>, Stephen J. Russell<sup>b</sup>, Kenneth Dalgarno<sup>a</sup>, Ana Marina Ferreira<sup>a,\*</sup>

<sup>a</sup> School of Mechanical and Systems Engineering, Newcastle University, Newcastle Upon Tyne, UK

<sup>b</sup> Nonwovens Research Group, School of Design, University of Leeds, Leeds, UK

## ARTICLE INFO

### Article history:

Received 17 September 2016

Accepted 12 March 2017

Available online 14 March 2017

### Keywords:

PHBV

Centrifugal spinning

Nanofibre

Microfibre

## ABSTRACT

This paper reports the first study on centrifugal spinning of PHBV fibres. Fibres were spun from solution using a range of polymer concentrations, spin speeds and spinneret to collector distances. A PHBV polymer concentration of 25% w/v spun at 9000 r min<sup>-1</sup> produced the highest quality fibres, with fibre diameters predominantly in the 0.5–3 µm range. The rate at which fibre could be produced at the 9000 r min<sup>-1</sup> spin speed and with a spinneret to collector distance of 39.2 cm was equivalent to 11 km of fibre per minute per needle. Average fibre strengths of 3 MPa were achieved, together with average moduli of 100 MPa, indicating that the fibres had higher strength but lower stiffness than electrospun PHBV. The productivity and mechanical properties achieved, together with the excellent biocompatibility of PHBV, means that these fibres have potential for application in a range of biomedical applications.

© 2017 The Authors. Published by Elsevier B.V. This is an open access article under the CC BY license (<http://creativecommons.org/licenses/by/4.0/>).

## 1. Introduction

Submicron fibrous assemblies have gained interest in the field of tissue engineering due to their large surface-area to volume ratio, high porosity and a structural similarity to extracellular matrix (ECM) [1,2]. Several ways are known to fabricate porous polymeric fibrous assemblies including phase separation, self-assembly and the most popular method, electrospinning [3]. Electrospinning is compatible with a relatively wide range of materials and produces nano and submicron fibres. However, in relation to the spinning of biopolymers for tissue scaffold production, the process has some limitations such as requirement of a high voltage electric field, solution conductivity and a relatively low productivity, which hinders its use for mass production of fibres [4]. Like electrospinning, the basic principles of centrifugal spinning have been industrially known for many years, such that the origins of the technology for processing naturally derived polymers can be traced back to at least the 1920s [5]. More recently, centrifugal spinning technology has been directed towards nanofibre web formation in an efficient, scalable, low-cost manner. During this process, inertial forces generated at high rotational speeds create and elongate a fluid solution or melt without the need for electrostatic stimulation [6]. In solution spinning, a high concentration polymeric solution is injected in to an integrated reservoir and spinneret. At high rotational speeds centrifugal forces cause a liquid jet to eject from the spinneret. Centrifugal and aerodynamic forces act to stretch and elongate the jet as the solvent evaporates, forming a solid filament or fibre. The fibres are then

collected onto static radial collectors or on to a vacuum conveyor [7,8]. Processing parameters such as the polymer concentration, solution viscosity, spinneret to collector distance and the spinneret rotation speed, influence fibre production and morphology [9]. Recently several studies have demonstrated the fabrication of micro/nano fibres using in-house centrifugal spinning systems, for example:

- Lu et al. [4] produced polyacrylonitrile fibres and investigated the effect spinning parameters had on fibre production.
- Ren et al. [3,6] produced micro and nanofibres from poly(L-Lactic acid) (PLLA) and polyvinylpyrrolidone (PVP).
- Wang et al. [10] used a system based on two cotton candy machines to create PLGA fibres using both melt and solvent assisted spinning, and Loordhuswamy et al. [9] who produced highly aligned polycaprolactone fibres.

The versatility of centrifugal spinning has created opportunities to produce fibres and webs of unique construction from biopolymers of interest in order to mimic the ECM and provide mechanical integrity. Polyhydroxyalkanoates (PHAs) are a class of thermoplastic polymer that is biocompatible and biodegradable, synthesised by microorganisms such as bacteria and haloarchaea. When an excess of carbon source is available PHAs are usually deposited as carbon and energy reserve materials [11]. One of the most extensively studied PHA's is Poly (3-hydroxy butyrate) (PHB), and its copolymer with hydroxyvalerate (HV). Altering the ratio of PHB to PHV facilitates tailoring of the physical characteristics and processability of the polymer [12] and incorporation of HV leads to an increase in chain flexibility and processability [12]. Poly (3-hydroxybutyrate-co-3-hydroxyvalerate) (PHBV) degrades *in vivo* to produce D-L-β-hydroxybutyrate, a normal constituent of human blood

\* Corresponding author at: School of Mechanical and Systems Engineering, Newcastle University, Claremont Road, Newcastle upon Tyne NE1 7RU, UK.  
E-mail address: [ana.ferreira-duarte@ncl.ac.uk](mailto:ana.ferreira-duarte@ncl.ac.uk) (A.M. Ferreira).

[13]. Owing to its natural derivation, favourable mechanical properties, biocompatibility, and degradation times, PHBV has been evaluated for use in various tissue engineering applications such as bone, cartilage, skin and nerve [14]. However, the adoption of centrifugal spinning as a method for producing PHBV fibres has not previously been investigated.

The objective of this study was to develop PHBV fibre webs via centrifugal spinning and to investigate the influence of processing parameters on fibre characteristics, including mechanical properties. The rotation speed, nozzle collector distance, polymer solution concentration and their effects on fibre morphology, mechanical properties and uniaxial thermal properties have been evaluated in order to establish processing conditions for reliable fibre production.

## 2. Materials and methods

Solutions of PHBV (12% Valerate, Sigma Aldrich UK) in chloroform (99.8% reagent grade, Sigma Aldrich UK), of concentrations 10, 15, 20 and 25% w/v, were prepared by dissolving PHBV pellets in chloroform in ambient conditions. The solutions were stirred for at least 12 h prior to use.

### 2.1. Rheological properties of the solutions

Changes in solution viscosity with increasing PHBV concentration were measured using a Brookfield DV-E dynamic rotational viscometer. A metallic cylinder was filled with 9.1 ml of polymeric solution. A spindle of type '31', supplied by Brookfield, was suspended in the solution and rotated at a given speed. The measured torque exerted on the spindle was converted in to shear stress which in turn was converted in to a viscosity value using a given spindle factor.

### 2.2. Centrifugal spinning parameters

A FibeRio (USA) 1000 M Forcespinning™ centrifugal spinning machine was used to produce the samples. A schematic of the machine layout is shown in Fig. 1. For each spin cycle, 1.6 ml of solution was injected in to a hollow fluid reservoir, which was tipped with two hypodermic needles (30 gauge with a shaft length of 12.5 mm). The collector was located radially to the spinneret and comprised a series of metallic bars at set distances of 29.6 cm (identified as ID) and 39.2 cm (identified as OD) from the spinneret. Cardboard rectangular frames of dimensions 180 mm and 85 mm were affixed to the bars to facilitate the collection of flat areas of fibrous web.

The solutions were processed at rotation speeds of 3000, 6000 and 9000  $\text{r min}^{-1}$ . For each spinning condition, two spins for 2 min, using 3.6 ml of solution per spin, were used to produce sufficient web mass for subsequent testing and evaluation.

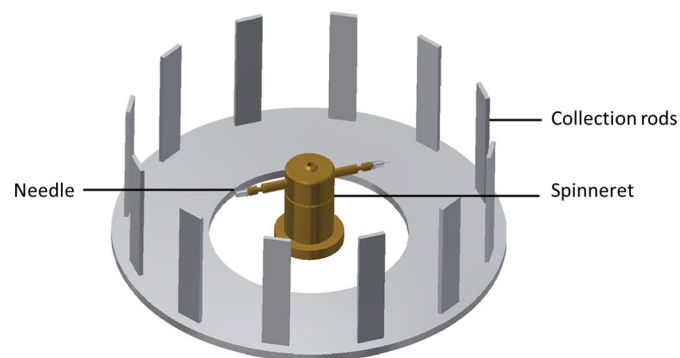


**Fig. 1.** Schematic representation of the FibeRio Forcespinning system: polymer solutions (15–25%) were fed into the rotating chamber in the middle of the system; rotation caused ejection of a jet of polymer solution from the two orifices (0.31 mm), with the fibres subsequently collected between the metal rods placed on the base.

### 2.3. Assessment of fibre morphology and diameter using scanning electron microscopy (SEM)

Specimens were coated with gold (15 nm) using a Polaron SEM Coating Unit and observed using SEM (TESCAN VEGA LMU, Newcastle University). The diameters of fibres ( $n = 20$ ) were measured from representative SEM images at  $1500\times$  magnification using ImageJ software. The procedure was repeated for  $n = 5$  different images for each spinning condition.

### 2.4. Thermal analysis

Differential scanning calorimetry (DSC) was used to investigate changes in the fine structure for selected PHBV webs with comparisons to the unprocessed pellet. Web and pellet samples (4–8 mg, aluminum pans) were analysed using a Perkin-Elmer JADE DSC. A heating scan from 0 to  $240\text{ }^{\circ}\text{C}$  was conducted at a rate of  $20\text{ }^{\circ}\text{C min}^{-1}$  under a nitrogen atmosphere.

### 2.5. Mechanical properties

Tensile tests were conducted using a Zwick Reoll 2010 (25 mm gauge length; crosshead speed  $1.67\text{ mm s}^{-1}$ ; 10 N load cell). Laser-cut cardboard C-frames of size  $30 \times 30\text{ mm}$  and frame thickness 5 mm were used as mounts for performing tensile measurements. Testing was performed in the machine direction of the webs, with the fibre webs oriented such that the circumferential fibre collection direction was the direction of loading. The webs were conditioned in an atmosphere of  $20 \pm 2\text{ }^{\circ}\text{C}$  and  $60 \pm 5\%$  RH. Sections of fibre web were cut and mounted on the C-frames using adhesive and clamped within the jaws of the tensile testing machine. The cardboard mount was then cut and the sample tested to failure. The weight of the fibre web was used to calculate an effective cross sectional area, which in turn was used to calculate stress and modulus.

## 3. Results

### 3.1. Viscosity of PHBV solutions

Fig. 2 shows that the viscosity of the PHBV solutions increased with increasing PHBV concentration. The viscosity increased from 35.0 cP at 10% to 386.2 cP at 25% PHBV concentration. As indicated in Fig. 2 measurements were a close fit ( $R^2 = 0.9968$ ) to an exponential curve, exhibiting the expected behaviour for a polymeric solution across a broad concentration range. The viscosity varied by an order of

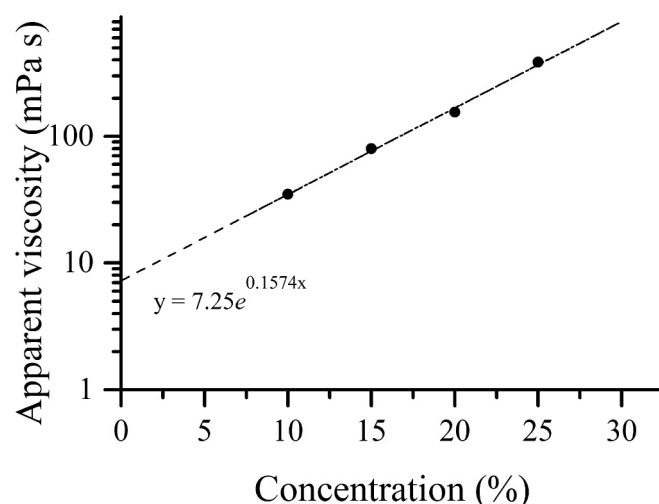


**Fig. 2.** Rotational viscosity measurements for PHBV solutions with exponential trendline.

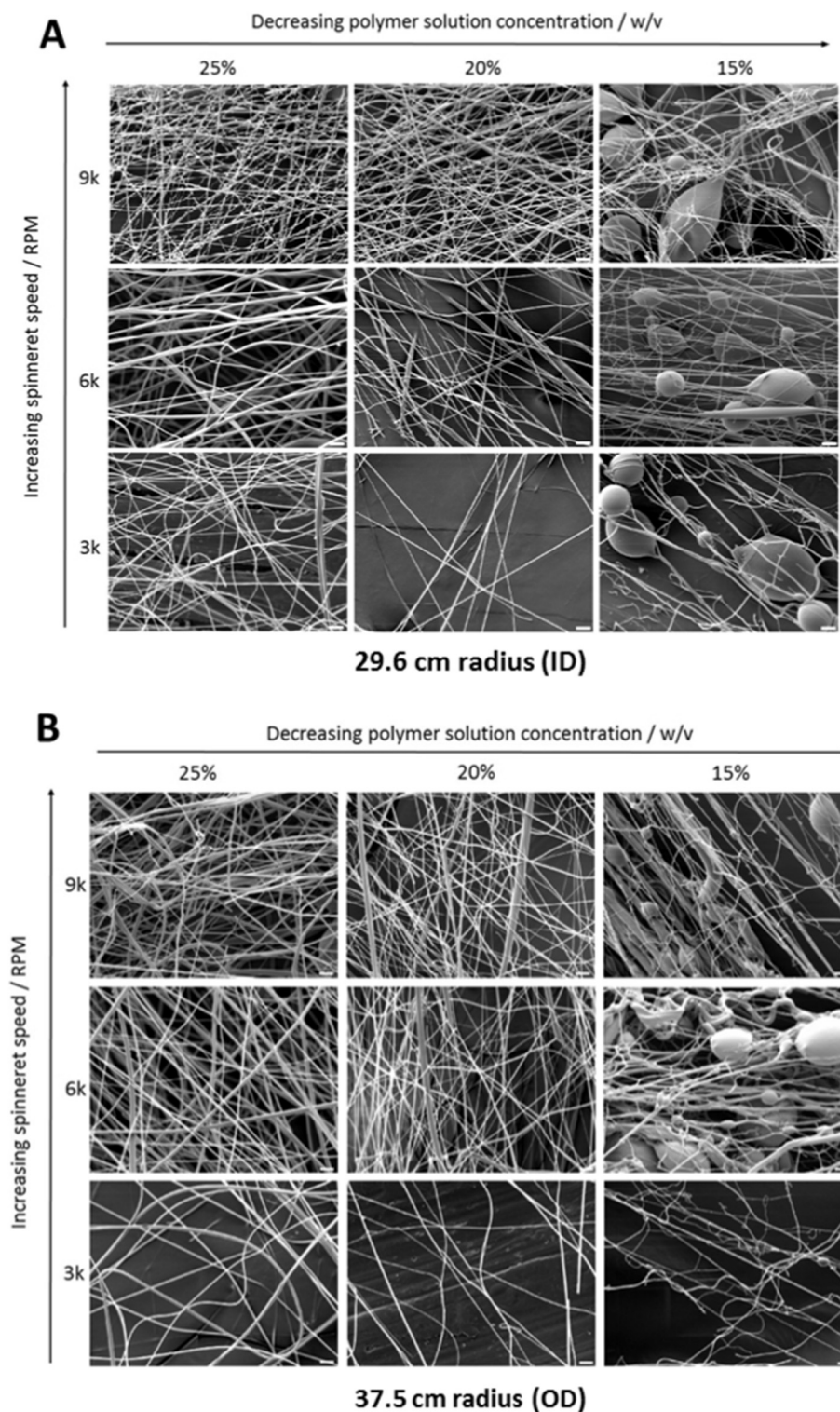
magnitude across the range of concentrations processed in the centrifugal spinner.

### 3.2. Fibre morphology and diameter

Fig. 3 shows fibre morphologies across the range of processing conditions, with Fig. 4 showing the variation in fibre diameter as determined from image analysis. In Fig. 3 it is evident that fibres produced

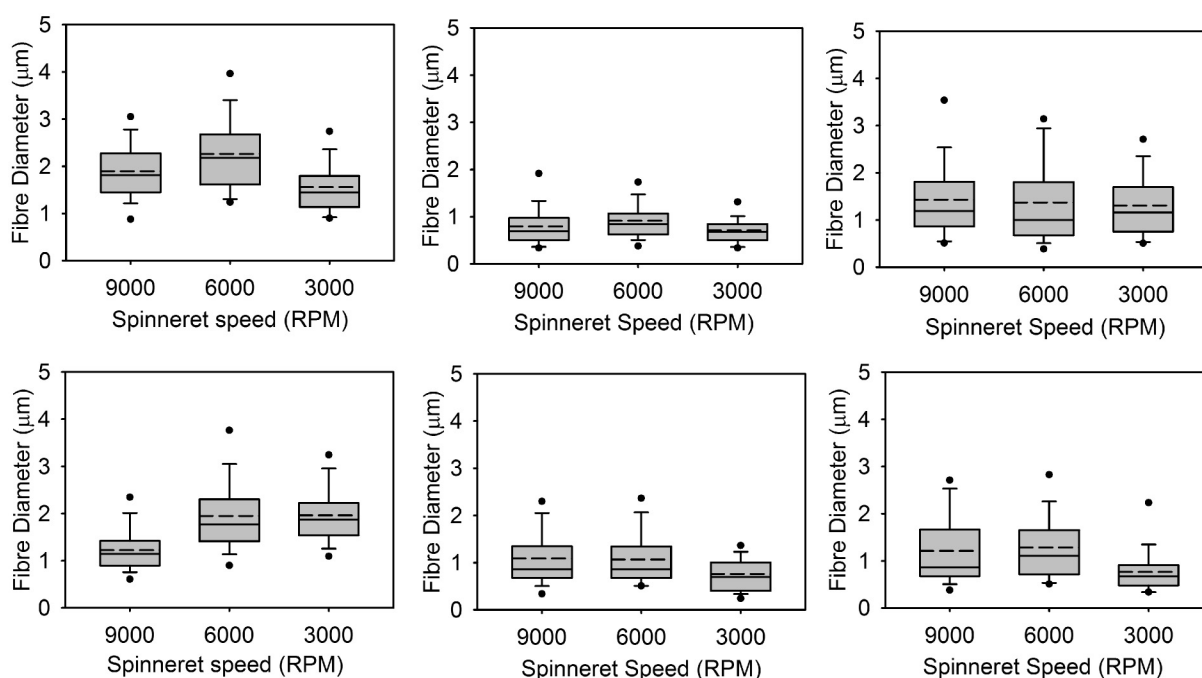
from the 15% w/v solution exhibited beading, shot formation and bead on string formation which was evident across the range of spinneret speeds and collection distances used, whereas the 20 and 25% w/v solutions produced uniform fibres free of beading. When a PHBV concentration of 10% w/v was spun, fibres were not continuous, were of poor quality and could not be collected.

Fig. 4 shows that the fibre diameters were predominantly in the 0.5 to 3  $\mu\text{m}$  range, with mean fibre diameters between 0.7 and 2.3  $\mu\text{m}$ . No



**Fig. 3.** SEM images showing variations in fibre morphology: A) collection distance ID 29.6 cm and B) collection distance OD. 37.5 cm, collected fibre webs produced at different combinations of spinneret rotation speed (3000, 6000 and 9000  $\text{rev min}^{-1}$ ) and polymer solution concentration (15, 20 and 25 w/v). Scale bars represents 5  $\mu\text{m}$ .





**Fig. 4.** Box plot of fibre diameters: left to right, 25, 20, 15% w/v; top ID 29.6 cm and bottom OD. 37.5 cm. Error bars represent the 95th and 5th quartiles, centre line is the median, dashed line is the mean.

marked trends in the variation of fibre diameter were evident as a result of changes in spinneret rotation speed, PHBV concentration or differences in the spinneret to collector distance. The best combination of productivity and fibre quality was considered to be achieved from processing 20 and 25% w/v solutions at 9000  $\text{r min}^{-1}$ .

### 3.3. Thermal analysis

DSC traces for selected PHBV fibres formed using the centrifugal spinning process are shown together with the DSC trace for unprocessed PHBV in Fig. 5. All the DSC traces revealed a primary melting point centred at 151.1 °C with a secondary peak between 133 °C and 140 °C. Double peaks of this form are normally indicative of multiple crystal forms within a material. For the PHBV pellet this secondary peak is significant in size and reaches a maxima at 139.1 °C. For the fibres, the size of this secondary peak is substantially reduced when compared to the pellet, and the peak apex shifts to around 133.7 °C. This shift was consistent for all of the fibres. Additionally, there was a reduction in enthalpy ( $\Delta H_m$ ) from 78.5  $\text{J g}^{-1}$  for the pellet, to values in the range 47–57  $\text{J g}^{-1}$  for the as-spun fibres.

### 3.4. Mechanical properties.

Fibres produced using 15% w/v PHBV solutions were too brittle to test, as were those spun from 20% w/v PHBV and collected at the OD. For fibres which were robust enough to test representative tensile curves and shown in Fig. 6, with the mean values for tensile strength, modulus and elongation at break given in Fig. 7.

The mechanical properties of the webs varied across tests, but fibre webs spun at 9000  $\text{r min}^{-1}$  were generally stronger and stiffer than those spun at the lower speeds, with fibres spun at 3000  $\text{r min}^{-1}$  generally more ductile than those spun at higher speeds. Fibres spun at 3000 and 6000  $\text{r min}^{-1}$  showed an increase in average strength and average modulus with increased spinneret to collector distance.

## 4. Discussion

### 4.1. Processability, morphology and productivity

Viscosities of between 100 and 300  $\text{mPa} \cdot \text{s}$  were found to be processable to create relatively uniform and coherent fibres across the range of spinneret rotation speeds and collection distances used in this work. At the highest rotation speed, collecting at the OD, the processing

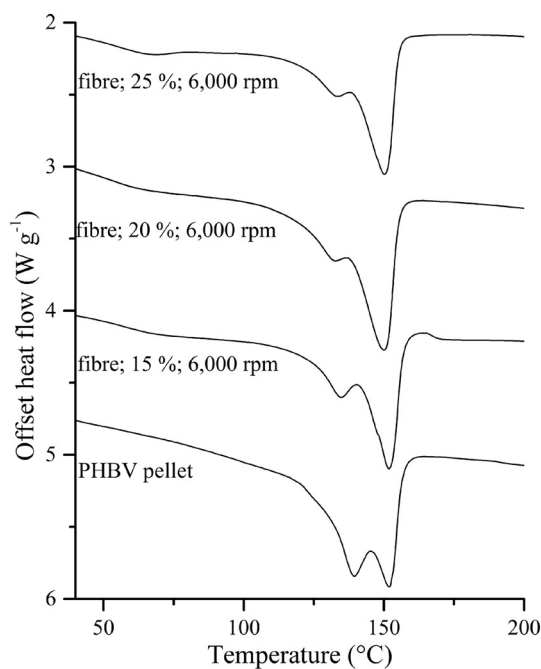


**Fig. 5.** DSC traces for PHBV pellet and PHBV fibres produced at a spinneret to collector distance of 29.6 cm and a rotation speed of 6000  $\text{r min}^{-1}$  for PHBV polymer concentrations of 15, 20 and 25% w/v.

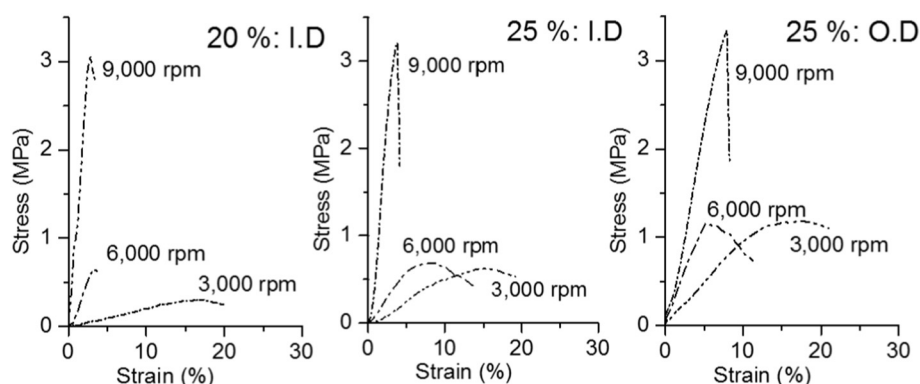


Fig. 6. Tensile curves for PHBV webs formed from 25% PHBV solutions.

conditions equate to a productivity of around 11 km of fibre per min per needle.

Analysis of the SEM images and fibre diameter measurements show that successful fibre production and resulting morphology varies with the starting PHBV polymer viscosity, a dependency well documented in the literature [15,16]. Previous work has linked increases in polymer solution concentration to the successful formation of continuous fibres with less beading [3], and has suggested that the increase in polymer loading is required in order to provide a sufficient density of polymer chain entanglements for a fibre to form, which would explain why the results at 20% and 25% w/v PHBV produced the best fibres. The beads-on-string morphology observed in Fig. 2 is well known within the electrospinning and centrifugal spinning literature [13,14] and is caused by Rayleigh instabilities resulting from an imbalance in viscosity and surface tension.

Fibre morphology is influenced by the evaporation rate of the solvent during spinning, which in-turn is linked to the distance between the spinneret tip and the collector during fibre formation. The closer the collection radius is, the shorter the stream time of the polymer liquid jet and the less time is available for adequate solvent evaporation. These results suggest that a collection radius of 29.6 cm allows evaporation of the solvent to occur, as no substantial decrease in mean fibre diameter was observed on increasing the collection radius.

The variability in fibre diameter may be related to variations in the volume of material during the force spinning process. Variations in the fluid fill level due to the continuous material feeding changes the pressure within the container, which is linked to the mass of fluid present [17]. In this work, 3.6 ml of solution was initially inserted into the

spinneret, but clearly in the absence of a continuous replenishing feed, the mass of fluid gradually reduces as the spinning process progresses.

#### 4.2. Thermal analysis

PHBV is novel among random copolymers as the hydroxy-valerate units can be accommodated within the hydroxy-butyrate crystal structure if the ratio of hydroxyl valerate is lower than 50 mol%. The PHBV grade used here contains 12% wt/wt valerate units and so it is expected that the HV elements are incorporated in to the HB crystal structure [18]. PHBV is known to form two crystal conformations: the  $\alpha$  orthorhombic cell and the  $\beta$  planar zigzag [19]. The double peak observed in the DSC scans is likely indicative of such  $\alpha$  and  $\beta$  crystal forms within the PHBV material [20].

The processing of PHBV into fibres shifts the position and magnitude of the secondary peak, linked to the  $\beta$  zigzag structure. A decrease in overall enthalpy and a decrease in secondary peak intensity have also been observed in electrospinning 12% valerate PHBV [21]. The high shear forces and rapid solidification induced during spinning are likely to disrupt the packing and crystallisation behaviour of the crystals, reducing the overall crystallinity along with favouring  $\alpha$  crystal formation [22]. This means that the  $\beta$  crystals are less numerous and smaller which can be seen in the apex of the secondary peak decreasing from 139 °C to 134 °C with spinning.

#### 4.3. Mechanical properties

The fibrous webs produced from the 20% w/v and 25% w/v PHBV solutions were suitable for mechanical testing because of their ease of

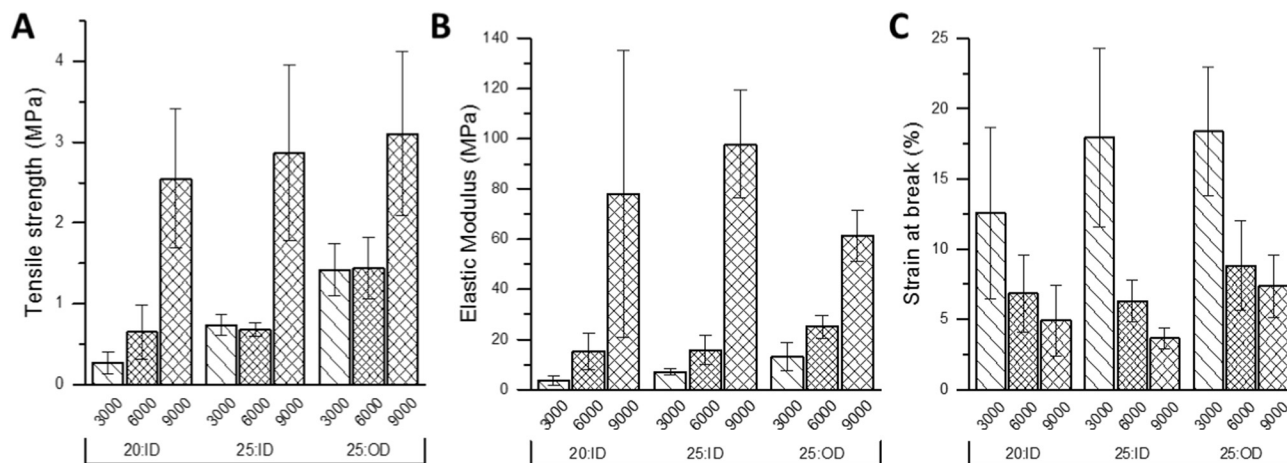


Fig. 7. Variations in the mean A. tensile strength, B. strain at break, and C. elastic modulus with spinneret rotation speed and spinneret to collector distance. Error bars indicate standard deviation.

handling and qualitative coherency. The coherence of these fibres is considered to be related to the generation of polymer chain entanglements during in-flight fibre formation.

The changes in tensile strength, strain at break, and modulus observed for different processing conditions are considered to be related to the degree of fibre orientation and fibre entanglement present within the webs, behaviour which is commonly observed for nonwovens [23]. The results in Figs. 6 and 7 suggest that increasing the rotational speed to  $9000 \text{ r min}^{-1}$  imparted a notably higher average stiffness and average tensile strength to the fibrous mats, and a lower average strain at break. The webs were tested only in the machine direction which is parallel with the direction of rotation. An increase in processing speed is considered to increase the fibre orientation in radially collected webs. At lower rotational speeds the fibres are deposited with less orientation in the direction of rotation and when subsequently tested the fibres within the webs can displace and rotate to align themselves with the load before failing. Alongside fibre alignment an increase in polymer orientation within the fibres could make a secondary contribution to the changes in mechanical properties. At higher rotational speeds there is significantly more drawing force on filaments as they form into fibres which will act to align the chains along the fibre axis. When loaded these fibres will be less extensible as the chains are already aligned in the direction of tension, increasing fibre strength and stiffness, which translates to improved properties of the web. The variability in the data is considered to be partly a result of the stochastic nature of testing nonwoven webs.

It is instructive to compare the tensile strength values of the as-spun PHBV fibres produced in the present study with those previously produced by electrospinning. For electrospun PHBV fibres Kuppan et al. [18] reported average tensile strengths of 1.4 MPa, and an average modulus of 1028 MPa, whilst Suwontang et al. [11] indicated average tensile strengths of 1.76 MPa, and average modulus of 125.7 MPa. The mechanical properties of fibre webs produced in this work by centrifugal spinning at  $9000 \text{ r min}^{-1}$  were strengths of 3 MPa on average, together with an average modulus of 100 MPa, indicating that the mechanical properties of the fibre webs produced by centrifugal spinning are of the same order as those previously reported for electrospun PHBV, with greater tensile strength but lower stiffness.

## 5. Conclusions

A Fibernio™ centrifugal spinning system was used to produce Ultra-fine fibrous mats of PHBV quickly and efficiently, with an effective production rate of 11 km of fibre per minute per needle at the highest spin speed. The morphology of the fibres produced was dependent on solution concentration and viscosity, and the rotational speed of the spinneret. Defect-free fibres were produced from polymer solutions at 20 and 25% w/v, with the best mechanical properties achieved through spinning the 25% w/v solution at 9000 rpm.

## Acknowledgements

This work was partly funded by the EPSRC Centre for Innovation in Medical Devices (MeDe Innovation; EP/K029592/1). We gratefully

acknowledge the support of the Clothworkers' Centre for Textile Materials Innovation for Healthcare in Leeds. The authors would like to thank Kath White and Tracey Davis at Newcastle University Electron Microscopy Research Services for their kind support with the fibres imaging.

## References

- [1] S. Heydarkhan-Hagvall, et al., Three-dimensional electrospun ECM-based hybrid scaffolds for cardiovascular tissue engineering, *Biomaterials* 29 (19) (2008) 2907–2914.
- [2] A. Khademhosseini, J.P. Vacanti, R. Langer, *Progress in tissue*, *Sci. Am.* 300 (5) (2009) 64–71.
- [3] L. Ren, et al., Large-scale and highly efficient synthesis of micro- and nano-fibers with controlled fiber morphology by centrifugal jet spinning for tissue regeneration, *Nano* 5 (6) (2013) 2337–2345.
- [4] Y. Lu, et al., Parameter study and characterization for polyacrylonitrile nanofibers fabricated via centrifugal spinning process, *Eur. Polym. J.* 49 (12) (2013) 3834–3845.
- [5] R.F. Allen, *Method of Making Fibers*, 1920 (Google Patents).
- [6] L. Ren, et al., Highly efficient fabrication of polymer nanofiber assembly by centrifugal jet spinning: process and characterization, *Macromolecules* 48 (8) (2015) 2593–2602.
- [7] M. Yanilmaz, X. Zhang, Polymethylmethacrylate/polyacrylonitrile membranes via centrifugal spinning as separator in Li-ion batteries, *Polymer* 7 (4) (2015) 629.
- [8] T. O'Haire, et al., Influence of nanotube dispersion and spinning conditions on nanofibre nanocomposites of polypropylene and multi-walled carbon nanotubes produced through Forcespinning™, *J. Thermoplast. Compos. Mater.* 27 (2) (2014) 205–214.
- [9] A.M. Loordhuswamy, et al., Fabrication of highly aligned fibrous scaffolds for tissue regeneration by centrifugal spinning technology, *Mater. Sci. Eng. C* 42 (2014) 799–807.
- [10] L. Wang, et al., Fabrication of polymer fiber scaffolds by centrifugal spinning for cell culture studies, *Microelectron. Eng.* 88 (8) (2011) 1718–1721.
- [11] D. Jendrossek, D. Pfeiffer, New insights in the formation of poly(hydroxyalkanoate) granules (carbonosomes) and novel functions of poly(3-hydroxybutyrate), *Environ. Microbiol.* 16 (8) (2014) 2357–2373.
- [12] K. Sombatmanikhong, et al., Bone scaffolds from electrospun fiber mats of poly(3-hydroxybutyrate), poly(3-hydroxybutyrate-co-3-hydroxyvalerate) and their blend, *Polymer* 48 (5) (2007) 1419–1427.
- [13] O. Suwantong, et al., In vitro biocompatibility of electrospun poly(3-hydroxybutyrate) and poly(3-hydroxybutyrate-co-3-hydroxyvalerate) fiber mats, *Int. J. Biol. Macromol.* 40 (3) (2007) 217–223.
- [14] G.-Q. Chen, Q. Wu, The application of poly(hydroxyalkanoates) as tissue engineering materials, *Biomaterials* 26 (33) (2005) 6565–6578.
- [15] P. Firbas, A. Seiber, Y.B. Cheng, Creation of titanium and zirconium carbide fibers with the forcespinning technique, *Int. J. Appl. Ceram. Technol.* 13 (4) (2016) 619–628.
- [16] W.-M. Chang, C.-C. Wang, C.-Y. Chen, The combination of electrospinning and forcespinning: effects on a viscoelastic jet and a single nanofiber, *Chem. Eng. J.* 244 (2014) 540–551.
- [17] S. Padron, et al., Experimental study of nanofiber production through forcespinning, *J. Appl. Phys.* 113 (2) (2013) 024318.
- [18] A. Bianco, M. Calderone, I. Cacciotti, Electrospun PHBV/PEO co-solution blends: microstructure, thermal and mechanical properties, *Mater. Sci. Eng. C* 33 (3) (2013) 1067–1077.
- [19] Q. Liu, et al., Poly (3-hydroxybutyrate) and poly (3-hydroxybutyrate-co-3-hydroxyvalerate): structure, property, and fiber, *Int. J. Polym. Sci.* 2014 (2014).
- [20] K.L. Dagnon, et al., Layer double hydroxides for enhanced poly (3-hydroxybutyrate-co-3-hydroxyvalerate) crystallization, *J. Appl. Polym. Sci.* 127 (5) (2013) 3395–3406.
- [21] C. Del Gaudio, et al., Assessment of poly ( $\epsilon$ -caprolactone)/poly (3-hydroxybutyrate-co-3-hydroxyvalerate) blends processed by solvent casting and electrospinning, *Mater. Sci. Eng. A* 528 (3) (2011) 1764–1772.
- [22] W.J. Orts, et al., Observation of strain-induced  $\beta$  form in poly ( $\beta$ -hydroxyalkanoates), *Macromolecules* 23 (26) (1990) 5368–5370.
- [23] M. Tausif, et al., Three-dimensional fiber segment orientation distribution using X-ray microtomography, *Microsc. Microanal.* 20 (04) (2014) 1294–1303.